# TorsinA restoration in a mouse model identifies a critical therapeutic window for DYT1 dystonia

Jay Li, Daniel S. Levin, Audrey J. Kim, Samuel S. Pappas, William T. Dauer

**Research Article**   **Neuroscience**

In inherited neurodevelopmental diseases, pathogenic processes unique to critical periods during early brain development may preclude the effectiveness of gene modification therapies applied later in life. We explored this question in a mouse model of DYT1 dystonia, a neurodevelopmental disease caused by a loss-of-function mutation in the *TOR1A* gene encoding torsinA. To define the temporal requirements for torsinA in normal motor function and gene replacement therapy, we developed a mouse line enabling spatiotemporal control of the endogenous torsinA allele. Suppressing torsinA during embryogenesis caused dystonia-mimicking behavioral and neuropathological phenotypes. Suppressing torsinA during adulthood, however, elicited no discernible abnormalities, establishing an essential requirement for torsinA during a developmental critical period. The developing CNS exhibited a parallel "therapeutic critical period" for torsinA repletion. Although restoring torsinA in juvenile DYT1 mice rescued motor phenotypes, there was no benefit from adult torsinA repletion. These data establish a unique requirement for torsinA in the developing nervous system and demonstrate that the critical period genetic insult provokes permanent pathophysiology mechanistically delinked from torsinA function. These findings imply that to be effective, torsinA-based therapeutic strategies must be employed early in the course of DYT1 dystonia.

**Find the latest version:**

https://jci.me/139606/pdf

# TorsinA restoration in a mouse model identifies a critical therapeutic window for DYT1 dystonia

Jay Li,[1,2] Daniel S. Levin,[3] Audrey J. Kim,[4] Samuel S. Pappas,[4,5] and William T. Dauer[4,5,6]

[1]Medical Scientist Training Program, [2]Cellular and Molecular Biology Graduate Program, [3]Department of Neurology, University of Michigan, Ann Arbor, Michigan, USA. [4]Peter O'Donnell Jr. Brain Institute,

[5]Department of Neurology, [6]Department of Neuroscience, University of Texas Southwestern Medical Center, Dallas, Texas, USA.

In inherited neurodevelopmental diseases, pathogenic processes unique to critical periods during early brain development may preclude the effectiveness of gene modification therapies applied later in life. We explored this question in a mouse model of DYT1 dystonia, a neurodevelopmental disease caused by a loss-of-function mutation in the *TOR1A* gene encoding torsinA. To define the temporal requirements for torsinA in normal motor function and gene replacement therapy, we developed a mouse line enabling spatiotemporal control of the endogenous torsinA allele. Suppressing torsinA during embryogenesis caused dystonia-mimicking behavioral and neuropathological phenotypes. Suppressing torsinA during adulthood, however, elicited no discernible abnormalities, establishing an essential requirement for torsinA during a developmental critical period. The developing CNS exhibited a parallel "therapeutic critical period" for torsinA repletion. Although restoring torsinA in juvenile DYT1 mice rescued motor phenotypes, there was no benefit from adult torsinA repletion. These data establish a unique requirement for torsinA in the developing nervous system and demonstrate that the critical period genetic insult provokes permanent pathophysiology mechanistically delinked from torsinA function. These findings imply that to be effective, torsinA-based therapeutic strategies must be employed early in the course of DYT1 dystonia.

## Introduction

During critical periods, the normally developing nervous system is uniquely sensitive to sensory stimuli that drive circuit plasticity. A unique landscape of molecular and circuit activities is responsible for critical periods. This special landscape also renders the maturing nervous system vulnerable to specific insults and receptive to particular therapeutic interventions.

A limited number of examples of critical period vulnerability to a pathogenic insult have been defined in mouse models of disease. Embryonic deletion of the Angelman syndrome protein *Ube3a* causes abnormal mouse behavioral phenotypes, whereas removal from juvenile (3 weeks old) or adult (12 weeks old) mice does not significantly influence behavior (1). A selective developmental window of vulnerability to neurodegeneration exists for ethanol exposure, corresponding to the period of rapid synaptogenesis (2, 3). Sensitivity to *Smn1* loss in spinal muscular atrophy models is exclusive to an early developmental period prior to the maturation of neuromuscular synapses (4). Beyond simply delineating critical periods of vulnerability, these studies illustrate how such efforts can improve understanding of disease pathogenesis by linking pathogenic insults to specific neurodevelopmental processes. Some neurodevelopmental diseases impair the CNS without temporal selectivity, however. Loss of *MeCP2* in mice produces Rett syndrome phenotypes whether initiated during early development or in adulthood (5).

Early pathogenic events that selectively disrupt developmental processes can produce a cascade of events that cause permanent circuit dysfunction mechanistically distinct from the initial insult. Paralleling the period of vulnerability, juvenile reexpression of *Ube3a* expression rescues a broad range of behavioral phenotypes in Angelman syndrome models — but adult reexpression is much less efficacious (6). Analogous to *MeCP2* inducing abnormal phenotypes when deleted from juvenile or adult mice, genetic restoration at any age is efficacious (7).

Dystonia is a CNS disease that manifests as abnormal, involuntary twisting. Considerable evidence implicates striatal dysfunction in dystonia pathogenesis (8–12). The natural history of DYT1 dystonia, an inherited form of the disease, strongly suggests a critical period of vulnerability, but this question has not been tested experimentally. The disease is incompletely penetrant, with only approximately one-third of mutation carriers developing symptoms (13, 14). Symptom onset typically occurs between 6 and 12 years of age. Critically, mutation carriers that do not develop symptoms as juveniles typically remain symptom-free for life (known as nonmanifesting carriers, ref. 15). These clinical data indicate that the DYT1 mutation selectively disrupts events essential for the maturation of motor circuits.

DYT1 dystonia is caused by a mutation in the *TOR1A* gene deleting a single glutamic acid residue (ΔE) from the torsinA protein (16). The ΔE mutation disrupts torsinA function through multiple mechanisms (17–21). Several in vivo studies suggest the existence of a critical period of CNS vulnerability to torsinA loss of function (LOF), but this question has never been explicitly addressed. These data have been collected in models in which torsinA was conditionally deleted from different parts of the CNS
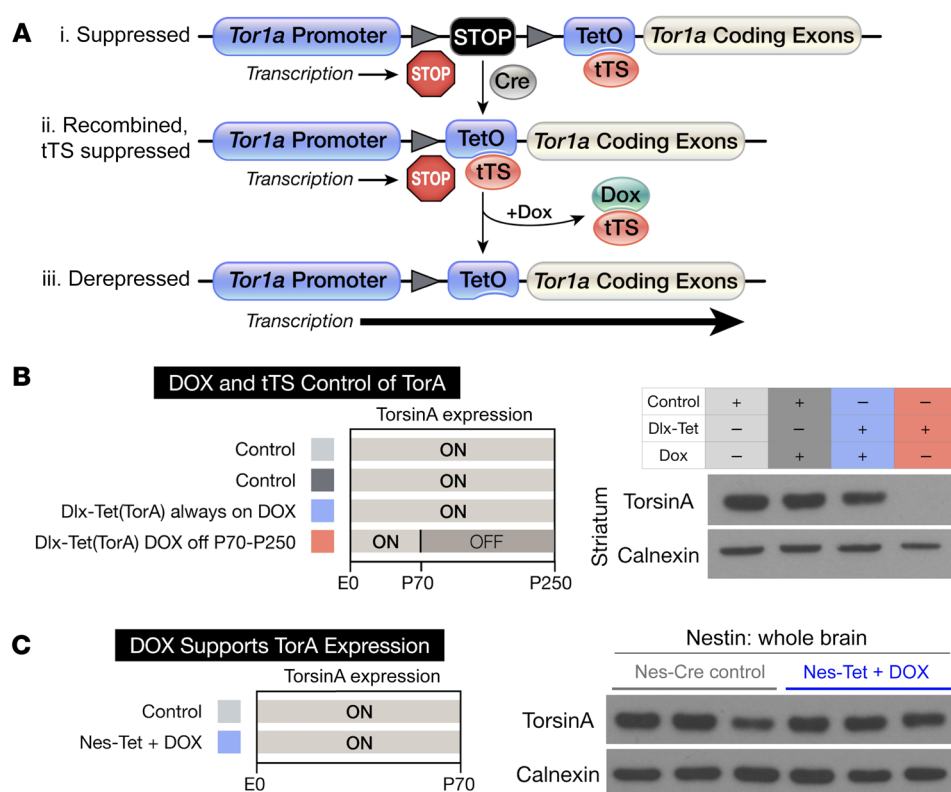
**Figure 1. Spatiotemporal control of the endogenous *Tor1a* locus.** (**A**) Design of the Tet(TorA) allele. Triangles denote loxP sites. (i) A "floxed-stop" cassette and TetO are inserted upstream of the start site of the *Tor1a* gene. (ii) Cre recombination removes the stop cassette, rendering the allele active specifically within the Cre expression field, unless suppressed by tTS. (iii) DOX derepresses the allele in the Cre expression field by preventing tTS binding to TetO, allowing transcription. (**B**) Western blot analysis of torsinA expression in striatal lysates from Dlx-Tet(TorA) mice. Light gray (ON) bars represent ages when torsinA is expressed and dark gray (OFF) areas represent ages when torsinA is suppressed. TorsinA is expressed in Dlx-Tet (TorA) mice fed DOX chow, but is suppressed in Dlx-Tet(TorA) mice switched to regular chow at P70 (compare lanes 3 and 4, with and without DOX). (**C**) Western blot analysis of torsinA expression in whole brain lysates from Nes-Tet(TorA) mice treated with DOX for their entire lives. DOX relieves tTS suppression, resulting in physiological levels of torsinA expression.

because construct-valid DYT1 dystonia model mice (i.e., *Tor1a*$^{\Delta E/+}$) do not exhibit motor abnormalities (22). The time course of cellular and behavioral phenotypes characteristic of these models is consistent with a unique role for torsinA in the developing CNS. These phenotypes emerge during late embryonic and early postnatal life but resolve in the first 3 to 4 postnatal weeks (23, 24). For example, nuclear membrane abnormalities develop in postmigratory, maturing neurons (17) but resolve in the first 3 postnatal weeks (24). Similarly, several of these models exhibit behavioral and neuropathological phenotypes that emerge during the first approximately 1 to 3 postnatal weeks but do not subsequently worsen and may even improve at later ages (17, 25, 26).

Here, we explicitly tested whether torsinA function is uniquely necessary during a neurodevelopmental critical period, and whether genetic rescue is similarly confined to an analogous therapeutic critical period. To rigorously address these questions, we developed a potentially novel mouse reagent that enabled spatiotemporal control of the endogenous torsinA allele. We found that in this system, embryonic suppression of torsinA caused overt dystonia-mimicking motor and neuropathological phenotypes. In contrast, torsinA suppression in adult mice (sustained for up to 6 months) caused no apparent behavioral or neuropathological abnormalities. TorsinA rescue of motor and neuropathological phenotypes similarly exhibited striking developmental dependence. Restoring torsinA expression in symptomatic juvenile mice reversed abnormal motor phenotypes and halted the progression of neuropathological change. In contrast, torsinA repletion during adulthood had no discernible effect. Our findings establish a requirement for torsinA function unique to an early critical period and suggest that torsinA-based therapeutics may need to be targeted early in the course of DYT1 dystonia.

## Results

*Cre- and tetracycline-based spatiotemporal control of the endogenous Tor1a locus.* To test for a torsinA critical period and explore whether torsinA repletion can reverse or suppress DYT1 phenotypes, we generated a mouse line that allowed control of the endogenous *Tor1a* locus. We created this line by targeting the endogenous *Tor1a* allele with a cassette that conferred Cre and tetracycline responsivity ("Tet[TorA]," ref. 27). This cassette, containing a "floxed stop" element followed by a tetracycline operator (TetO), was targeted just 5′ to the *Tor1a* start site (Figure 1A).

We first tested the ability of a tetracycline-controlled transcriptional silencer (tTS) to suppress torsinA expression from the Tet(TorA) allele and the ability of doxycycline (DOX) to displace tTS from the TetO sequence and enable gene expression (28). Our approach was based on Dlx-CKO (*Dlx5/6-Cre Tor1a*$^{flx/-}$) mice (12). The Dlx5/6-Cre field includes cortical inhibitory neurons, striatal cholinergic interneurons, striatal GABAergic interneurons, and medium spiny projection neurons (29), populations implicated in the corticostriatal circuit dysfunction underlying dystonic movements (30–32). We used the ubiquitously expressed *β-actin–tTS* allele (33) to generate *Dlx5/6-Cre Tor1a*$^{Tet/flx}$ *β-actin–tTS* mice, a model analogous to Dlx-CKO mice but using the new Tet(TorA) allele. In these animals, Cre selectively deleted the floxed *Tor1a* allele from all striatal neurons, as well as the floxed stop cassette within the Tet(TorA) allele. In this configuration, the Tet(TorA) allele should be suppressed by tTS, creating a *Dlx5/6-Cre* conditional null, but the allele should also be DOX regulatable selectively within the *Dlx5/6-Cre* field. We administered DOX to these animals from conception (in the mother's chow) until P70 to test its ability to maintain normal torsinA expression. We then withdrew

DOX at P70 to test the ability of tTS to suppress the Tet(TorA) allele (Figure 1B). P250 Dlx-Tet(TorA) mice continuously administered DOX displayed normal striatal torsinA expression. In contrast, torsinA expression was undetectable in P250 Dlx-Tet(TorA) mice switched to regular chow at P70. These results confirmed that the Tet(TorA) allele was efficiently suppressed by tTS, and that this suppression was relieved by DOX. Striatal levels of torsinA were essentially undetectable in Dlx-Tet(TorA) mice never administered DOX, further demonstrating the ability of tTS to effectively suppress the Tet(TorA) gene (Supplemental Figure 1, A and B; supplemental material available online with this article; https://doi.org/10.1172/JCI139606DS1). Comparing the expression of a single WT or Tet(TorA) allele in the absence of tTS demonstrate that they were expressed at comparable levels (compare *Dlx5/6-Cre Tor1a*[Tet/flx] and *Dlx5/6-Cre Tor1a*[flx/+] *β-actin–tTS* mice; Supplemental Figure 1, A and B). These findings demonstrate that the Tet(TorA) allele was expressed at levels indistinguishable from the WT *Tor1a* allele and efficiently suppressed by tTS.

We next tested the ability of DOX to derepress torsinA expression in the entire CNS in Nestin-Cre *Tor1a*[Tet/flx] β-actin–tTS ["Nes-Tet(TorA)"] mice, in which Cre was expressed throughout the CNS. DOX administration from gestation in Nes-Tet(TorA) mice maintained normal levels of whole-brain torsinA protein levels (Figure 1C and Supplemental Figure 1C). These data demonstrate that the Tet(TorA) allele was expressed normally and could be regulated throughout the CNS.

*TorsinA is essential during a critical period of vulnerability*. Dysfunction of corticostriatal circuits is strongly implicated in dystonia pathophysiology in human studies (8, 34, 35) and rodent studies (10–12, 36, 37). Dlx-CKO mice exhibit dystonic-like limb clasping and hyperactivity that emerges during the third postnatal week (12).

To explore whether these phenotypes depend upon torsinA LOF during a critical period of vulnerability, we compared the behavioral and histopathological effects of initiating suppression of torsinA expression in either developing or adult animals. We first tested whether initiating torsinA suppression prenatally replicates established Dlx-CKO phenotypes, including motor dysfunction during tail suspension and increased locomotor activity (12). tTS-mediated suppression of torsinA in Dlx5/6-Cre⁺ neurons starting in utero recapitulated the limb clasping and hyperactivity characteristic of Dlx-CKO mice (Figure 2, B and C). These data provide additional evidence that tTS suppressed torsinA levels to a similar degree as the conditional null allele (Supplemental Figure 1, A and B). To test the effect of initiating torsinA LOF in adulthood, we administered DOX to Dlx-Tet(TorA) mice from conception (in mother's chow) to maintain normal torsinA expression until P70. After P70, we withdrew DOX, allowing tTS to suppress the Tet(TorA) allele (Figure 2D). Western blots of striatal lysates confirmed the expected levels of torsinA protein (Figure 1B and Supplemental Figure 2). In marked contrast to initiating torsinA suppression in utero, adult suppression caused no behavioral abnormalities in any measures tested. Adult suppressed mice did not exhibit limb clasping or trunk twisting during tail suspension at any point during 6 months of longitudinal testing (Figure 2E). During this time, we observed no significant effects on locomotor activity (Figure 2F) or weight (Supplemental Figure 3A). We also assessed motor learning using the accelerating rotarod.

Adult suppressed mice did not differ from their nonsuppressed littermate controls in the rate at which they learned the task or the time they were able to remain on the rotarod (Supplemental Figure 3B). We confirmed that DOX itself did not exert an effect by administering DOX to Dlx-CKO mice (which lack any tetracycline-dependent alleles) from E0 to 6 months. DOX administration had no effect on the severity of limb clasping in Dlx-CKO mice (Supplemental Figure 4A).

Selective vulnerability during CNS development was similarly observed in histopathological studies of these animals. Suppressing torsinA in utero (Figure 3A) recapitulated the extent and pattern of cholinergic interneuron (ChI) loss previously observed in Dlx-CKO mice (refs. 12, 38 and Figure 3, B and C). In utero suppression also recapitulated the abnormal nuclear pore complex (NPC) clustering characteristic of Dlx-CKO mice (Figure 3D, Supplemental Figure 5A, and ref. 23). In striking contrast, adult torsinA suppression caused no discernible histopathological abnormalities. Despite lacking torsinA expression for nearly 6 months, the cortex and striatum of these animals were indistinguishable from their littermate controls (Supplemental Figure 6, A, C, and D). There was no evidence of reactive astrogliosis (Supplemental Figure 6B), and the number of striatal neurons (Supplemental Figure 6E) did not differ from littermate controls. Similarly, there were no changes in ChI number or NPC distribution (Figure 3, F–H, and Supplemental Figure 5B). We also confirmed that DOX itself did not exert an effect by administering DOX to Dlx-CKO mice (which lack any tetracycline-dependent alleles) from E0 to 6 months. DOX-treated Dlx-CKO mice exhibited the same severity of ChI degeneration as littermate Dlx-CKO mice fed regular chow (Supplemental Figure 4B). Considered together with the behavioral data, these observations demonstrate that the developing forebrain exhibits a critical period of susceptibility to torsinA LOF.

To explore whether the critical period demonstrated for the forebrain generalizes to other torsinA-sensitive brain regions, we used Nestin-Cre to modulate torsinA expression in the entire CNS. We first confirmed that suppression of the tetracycline-responsive allele in the Nestin-Cre field replicated the phenotypes established for conditional CNS deletion of the *Tor1a* allele using Nestin-Cre ("Nes-CKO," ref. 25). Nes-Tet(TorA) mice never administered DOX replicated all Nes-CKO phenotypes previously described, including early postnatal lethality (Figure 4, B and C). Nes-Tet(TorA) mice also exhibited abnormal postures similar to those reported for Nes-CKO mice (Supplemental Figure 7A, ref. 25). In striking contrast, Nes-Tet(TorA) mice that received DOX starting in utero were indistinguishable from their littermate controls. These animals exhibited normal viability (data not shown) and weight (Supplemental Figure 7, A and B), performed normally in all behavioral assays, and showed no evidence of any abnormal twisting movements (Supplemental Figure 7A, data not shown). To test the effect of initiating pan-CNS torsinA LOF in adulthood, we administered DOX to Nes-Tet(TorA) mice from conception (in mother's chow) to maintain normal torsinA expression until P70. After P70, we withdrew DOX, allowing tTS to suppress the Nes-Tet(TorA) allele (Figure 4D). We confirmed that DOX removal eliminated torsinA protein expression (Supplemental Figure 8, A and B). In striking contrast to the effects observed when torsinA suppression was initiated in utero, initiating torsinA suppression
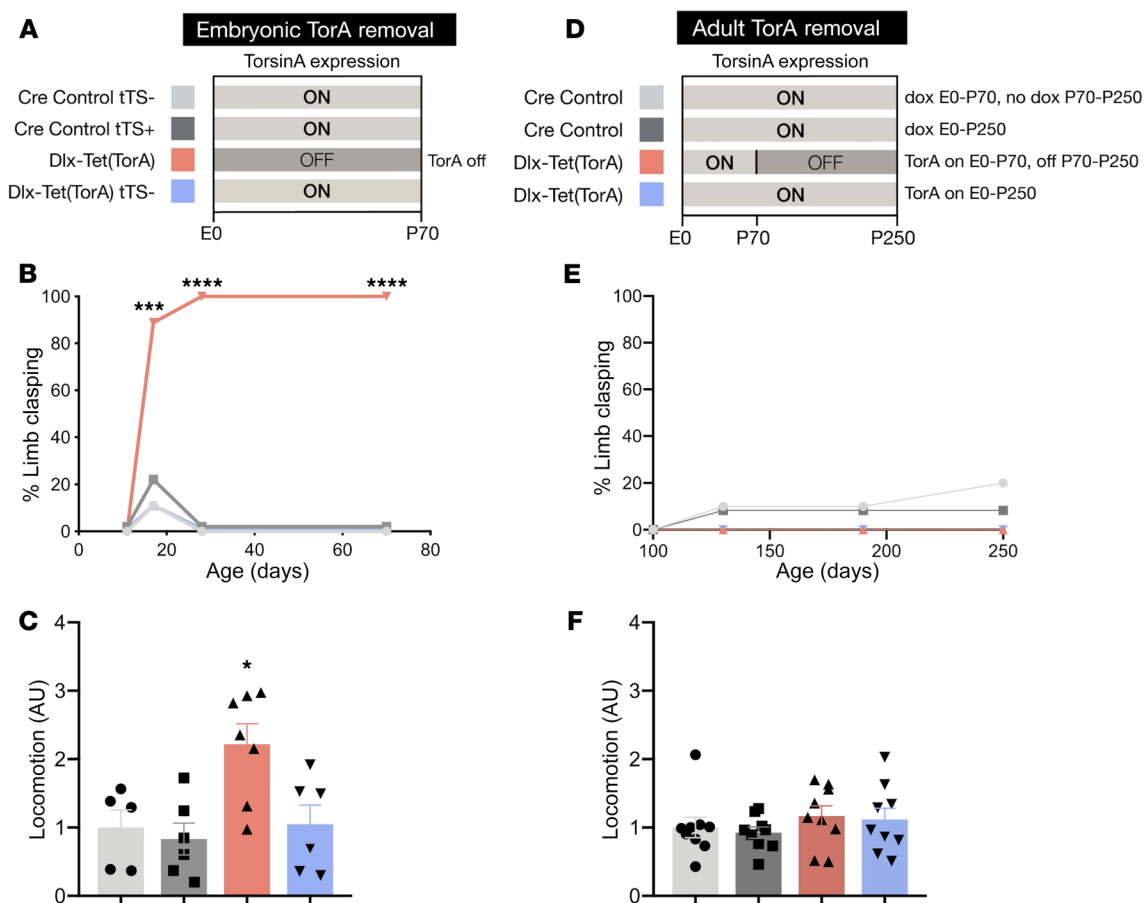
**Figure 2. Forebrain torsinA depletion causes abnormal limb clasping behavior only when initiated during CNS development.** (**A**) Schematic of experimental design for prenatal torsinA suppression in the Dlx5/6-Cre field. Light gray (ON) bars represent ages when torsinA is expressed and dark gray (OFF) areas represent ages when torsinA is suppressed. Each color corresponds to an experimental group in subsequent graphs. (**B**) Proportion of Dlx-Tet(TorA) mice exhibiting tail suspension–induced limb clasping (P17 to P70) after prenatal torsinA suppression. $n$ = 9–10 per group. (**C**) Locomotor activity of P70 Dlx-Tet(TorA) mice after prenatal torsinA suppression. These animals exhibit locomotor hyperactivity. $n$ = 5–7 per group. (**D**) Schematic of experimental design for adult torsinA suppression in the Dlx5/6-Cre field. Light gray (ON) bars represent ages when torsinA is expressed and dark gray (OFF) areas represent ages when torsinA is suppressed. Each color corresponds to an experimental group in subsequent graphs. TorsinA expression was suppressed by doxycycline withdrawal at P70. (**E**) Proportion of Dlx-Tet(TorA) mice exhibiting tail suspension–induced limb clasping after adult suppression of torsinA. Adult removal of torsinA in the forebrain does not cause limb clasping. $n$ = 10–12 per group. (**F**) Locomotor activity of Dlx-Tet(TorA) mice after adult suppression of torsinA. Adult removal of torsinA from the forebrain does not significantly alter locomotor activity. $n$ = 9 per group. Data analyzed by $\chi^2$ test (**B** and **E**), 1-way ANOVA (**C** and **F**), and Dunnett's multiple-comparison test (**C**). *$P < 0.05$, ***$P = 0.0004$, ****$P < 0.0001$.

in adulthood had no discernible effect on any measure examined, despite the fact that we observed the animals for up to 6 months after DOX removal. These animals exhibited normal weight (Figure 4E) and viability (all mice survived; data not shown) and performed similarly to controls in all behavioral tests, including locomotor activity in the open field, rotarod motor learning (Figure 4, F and G), and tail suspension (Figure 4H). We also tested for postural phenotypes reported in other torsinA LOF mouse models, including abnormal spinal curvature and overt dystonia (e.g., disrupted gait, falling over) in the open field (38, 39). No abnormal postural phenotypes were observed (Figure 4H). We also confirmed that whole-life DOX treatment itself had no effect on the behavioral phenotypes (including early lethality) of Nes-CKO mice (which lack any tetracycline-dependent alleles, Supplemental Figure 9), eliminating the possibility that torsinA-independent effects of DOX affect DYT1 phenotypes.

Neuropathological assessments of the brains of Nes-Tet (TorA) mice paralleled the behavioral findings. Initiating torsinA suppression in utero recapitulated all expected neuropathological phenotypes, whereas we observed no abnormalities when suppression was initiated in adulthood. The brains of Nes-Tet (TorA) mice that never received DOX (i.e., torsinA expression suppressed) exhibited reduced size (Figure 5A and Supplemental Figure 10, A–C) and astrogliosis in sensorimotor regions described previously for conditional CNS mutants (Figure 5, B and C; Supplemental Figure 10D; and ref. 25). Initiating DOX from conception (supporting torsinA expression) completely rescued these abnormalities (Supplemental Figure 7, C and D). Initiating torsinA suppression (by removing DOX) in adulthood (P70) did not cause any discernible neuropathological abnormalities. Six months after adult DOX withdrawal, the brains of these mice exhibited normal size and cortical thickness and no evidence of gliosis or neuro-
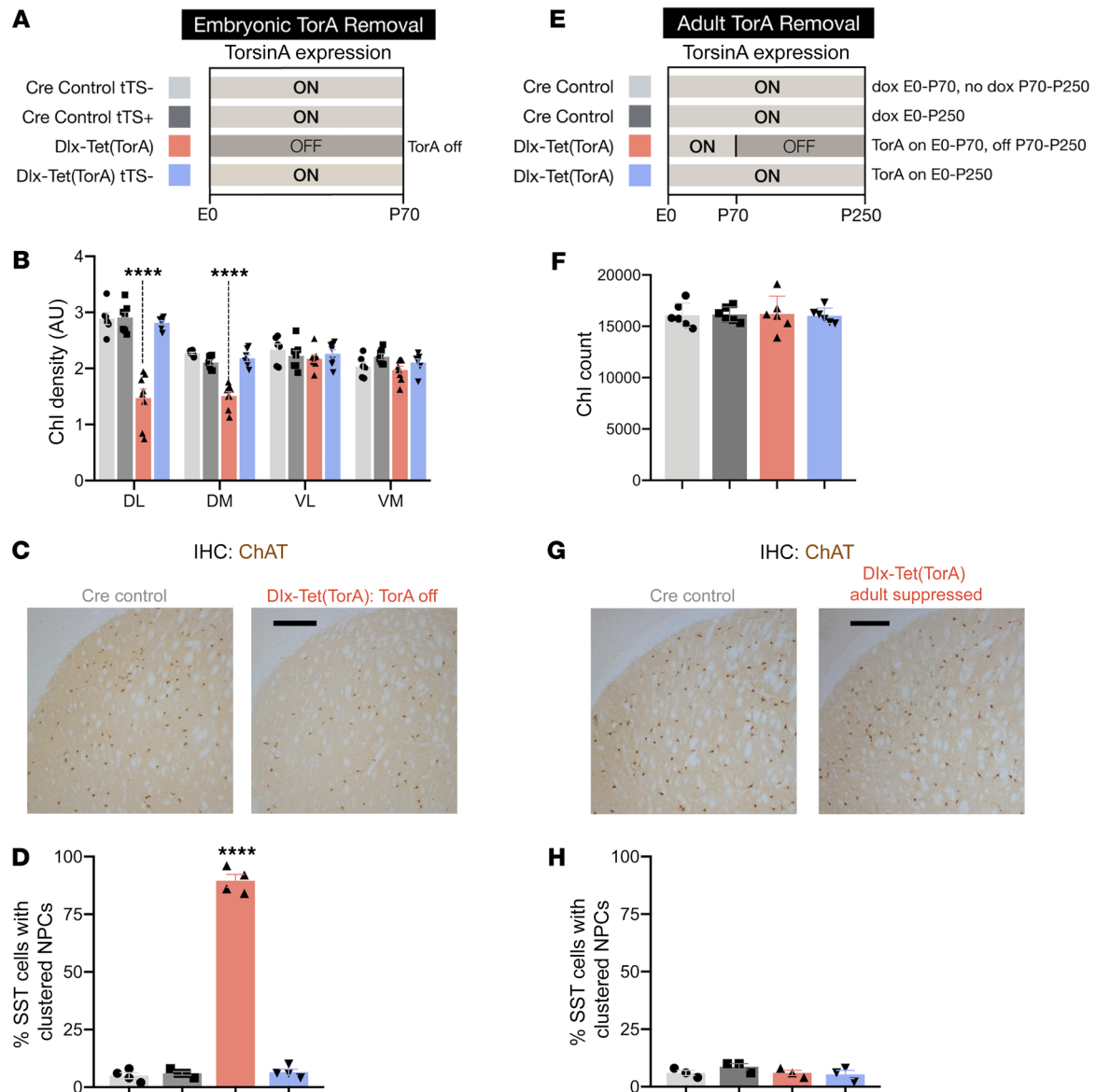
**Figure 3. Forebrain torsinA depletion causes neuropathology only when initiated during CNS development.** (**A**) Schematic of experimental design for prenatal torsinA suppression in the Dlx5/6-Cre field. Light gray (ON) areas of bars represent ages when torsinA is expressed and dark gray (OFF) areas represent ages when torsinA is suppressed. Each color corresponds to an experimental group in subsequent graphs. (**B**) ChI density analysis in 4 quadrants of caudate putamen (DL, dorsolateral; DM, dorsomedial; VL, ventrolateral; VM, ventromedial) in P70 Dlx-Tet(TorA) mice after prenatal torsinA suppression. Consistent with Dlx-CKO findings, Dlx-Tet(TorA) mice with torsinA removed at embryonic age exhibit ChI loss in dorsolateral and dorsomedial quadrants of caudate putamen. n = 6–8 per group. (**C**) Representative image of ChAT-stained striatum in Dlx-Tet(TorA) mice after prenatal torsinA suppression. Scale bar: 250 μm. (**D**) Percentage of SST+ neurons in sensorimotor cortex with clustered nuclear pore complexes in P70 Dlx-Tet(TorA) mice after prenatal torsinA suppression. n = 4 per group. (**E**) Schematic of experimental design for adult torsinA suppression in the Dlx5/6-Cre field. Light gray (ON) areas of bars represent ages when torsinA is expressed and dark gray (OFF) areas represent ages when torsinA is suppressed. Each color corresponds to an experimental group in subsequent graphs. TorsinA expression was suppressed by doxycycline withdrawal at P70. (**F**) Striatal ChI counts in Dlx-Tet(TorA) mice after adult suppression of torsinA. Adult forebrain suppression of torsinA does not cause ChI degeneration. (**G**) Representative image of ChAT-stained striatum in Dlx-Tet(TorA) mice after adult suppression of torsinA. Scale bar: 250 μm. (**H**) Percentage of SST+ neurons with abnormally clustered nuclear pore complexes in sensorimotor cortex of Dlx-Tet(TorA) mice after adult suppression of torsinA. Forebrain suppression of torsinA starting at P70 does not cause abnormal nuclear pore clustering. n = 4 per group. Data analyzed by 1-way ANOVA (**B** and **D**), Dunnett's multiple-comparison test (**B** and **D**), and 2-way ANOVA (**F** and **H**). ****$P < 0.0001$.

degeneration (Figure 5, E–H, and Supplemental Figure 11, A–C). These results demonstrate that all brain regions previously identified as susceptible to torsinA LOF exhibited a similar temporal torsinA requirement limited to early brain development. Considered together, our behavioral and histological assessment of mice with prenatal versus adult removal of torsinA from the entire CNS highlight a selective developmental susceptibility to torsinA LOF. Prenatal torsinA removal caused early lethality, impaired postnatal growth, and induced widespread neurodegeneration. On the other hand, extensive behavioral and histological analysis of mice
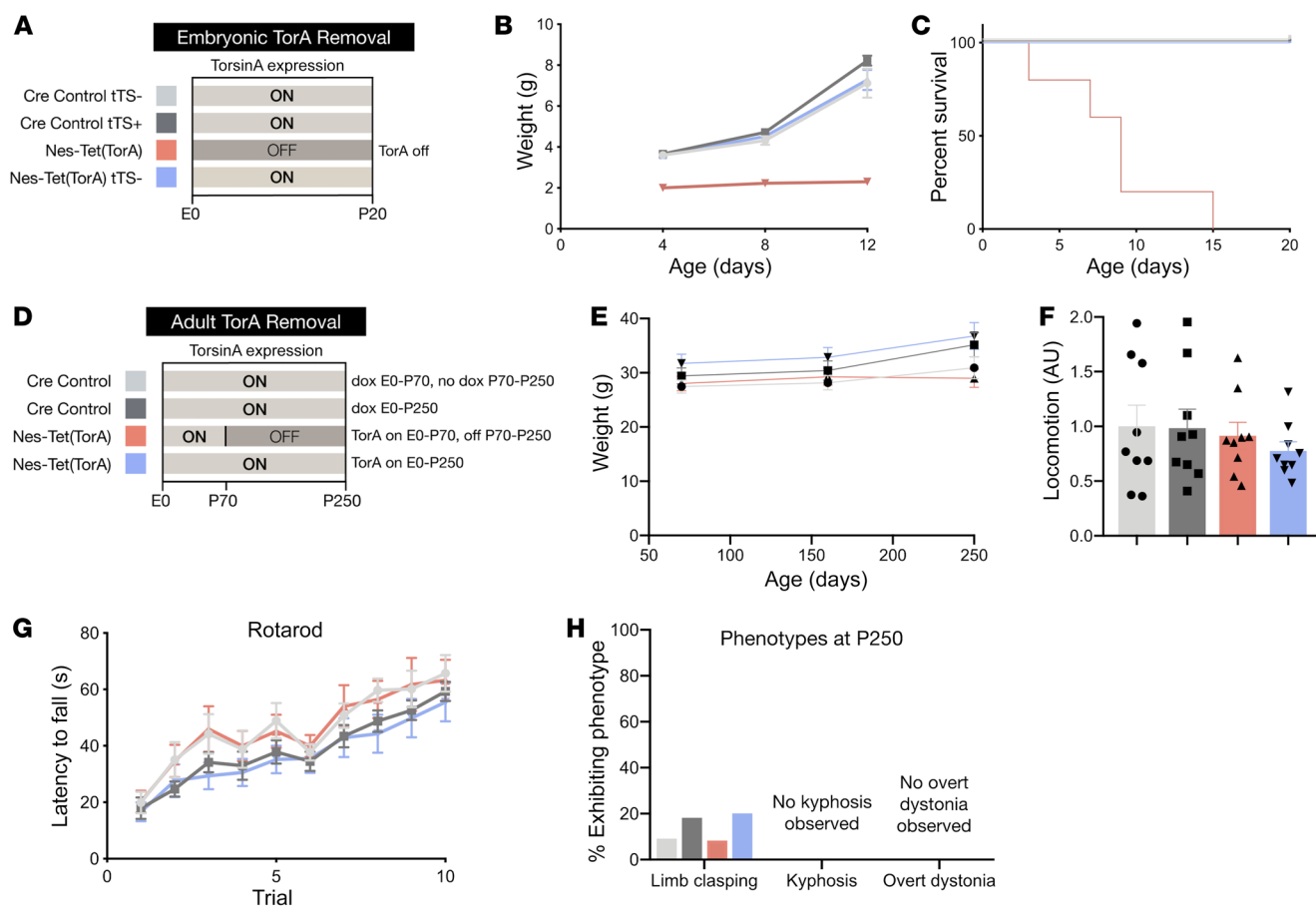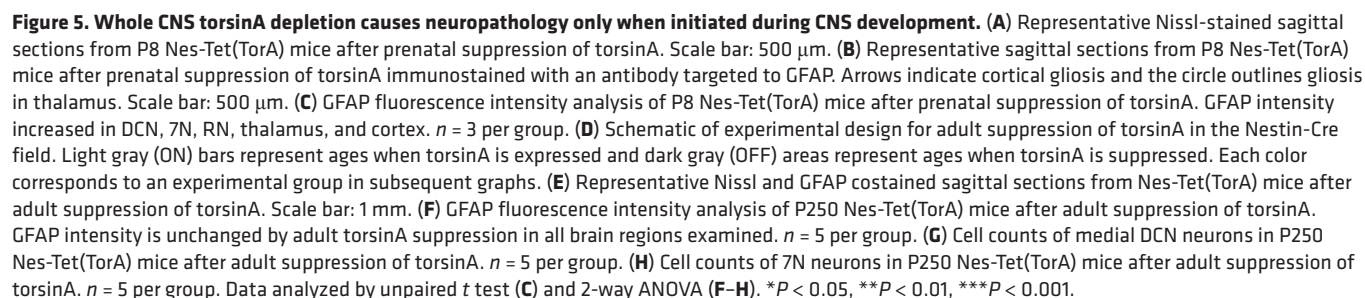
**Figure 4. Whole CNS torsinA depletion causes abnormal twisting behavior only when initiated during CNS development.** (**A**) Schematic of experimental design for prenatal suppression of torsinA in the Nestin-Cre field. Light gray (ON) bars represent ages when torsinA is expressed and dark gray (OFF) areas represent ages when torsinA is suppressed. Each color corresponds to an experimental group in subsequent graphs. (**B**) Growth curves of Nes-Tet(TorA) mice after prenatal suppression of torsinA. Embryonic torsinA removal impairs growth (interaction of age and experimental group: $P$ = 0.0026). $n$ = 4–5 per group. (**C**) Survival curves of Nes-Tet(TorA) mice after prenatal suppression of torsinA. Embryonic torsinA removal causes early lethality ($P < 0.0001$). $n$ = 5 per group. (**D**) Schematic of experimental design for adult suppression of torsinA in the Nestin-Cre field. Light gray (ON) bars represent ages when torsinA is expressed and dark gray (OFF) areas represent ages when torsinA is suppressed. Each color corresponds to an experimental group in subsequent graphs. TorsinA expression was suppressed by doxycycline withdrawal at P70. (**E**) Weight of Nes-Tet(TorA) mice after adult suppression of torsinA. (**F**) Locomotor activity of Nes-Tet(TorA) mice after adult suppression of torsinA. Adult suppression of torsinA does not alter locomotor activity. $n$ = 9 per group. (**G**) Rotarod performance of Nes-Tet(TorA) mice after adult suppression of torsinA. Adult forebrain suppression of torsinA does not impair motor learning. $n$ = 10–12 per group. (**H**) Percentage of motor phenotypes observed in other torsinA LOF models in Nes-Tet(TorA) mice after adult suppression of torsinA. Adult suppression of torsinA does not elicit torsinA-LOF–associated behavioral phenotypes such as limb clasping, kyphosis, and overt dystonic symptoms. $n$ = 10–12 per group for limb clasping and kyphosis. $n$ = 8 per group for analysis of overt dystonic symptoms. Data analyzed by mixed-effects model (**B**), Gehan-Breslow-Wilcoxon test (**C**), 2-way ANOVA (**E**–**G**), and $\chi^2$ test (**H**).

with adult torsinA removal from the same structures revealed no detectable phenotype.

*TorsinA restoration defines a therapeutic critical period for DYT1 dystonia.* A specific temporal requirement for torsinA implies that to be effective, torsinA restoration strategies may similarly need to be administered during a neurodevelopmental window. We tested for such a therapeutic critical period by initiating torsinA expression (by DOX administration) at different ages in mice that developed in the absence of torsinA (i.e., had never previously received DOX). We pursued these studies in Dlx-Tet(TorA) mice that, in the absence of DOX, developed abnormal twisting movements during the third postnatal week (Figure 2B and ref. 12). To model intervention during early disease, we induced torsinA expression at P21, approximately 1 week after the onset of abnormal limb clasping

(Figure 6A). To model intervention in chronic disease, we induced torsinA expression at P70, approximately 7 weeks after the onset of motor abnormalities (Figure 6B). DOX administration efficiently activated torsinA expression at both time points (Supplemental Figure 12, A–D). TorsinA restoration at P21 significantly reduced the duration of abnormal limb clasping by approximately 75% (Figure 6C; assessed at P70). In contrast, activating torsinA at P70 had no significant effect on the duration of limb clasping at any subsequent age tested, up to P168 (Figure 6D). We pursued histopathological analyses to determine whether ChI degeneration, which is linked to abnormal twisting behavior (12), paralleled the behavioral findings. TorsinA restoration at P21 significantly attenuated ChI loss, whereas P70 restoration produced no significant effect (Figure 6, E and F). The significant (but partial) rescue of neurodegen-
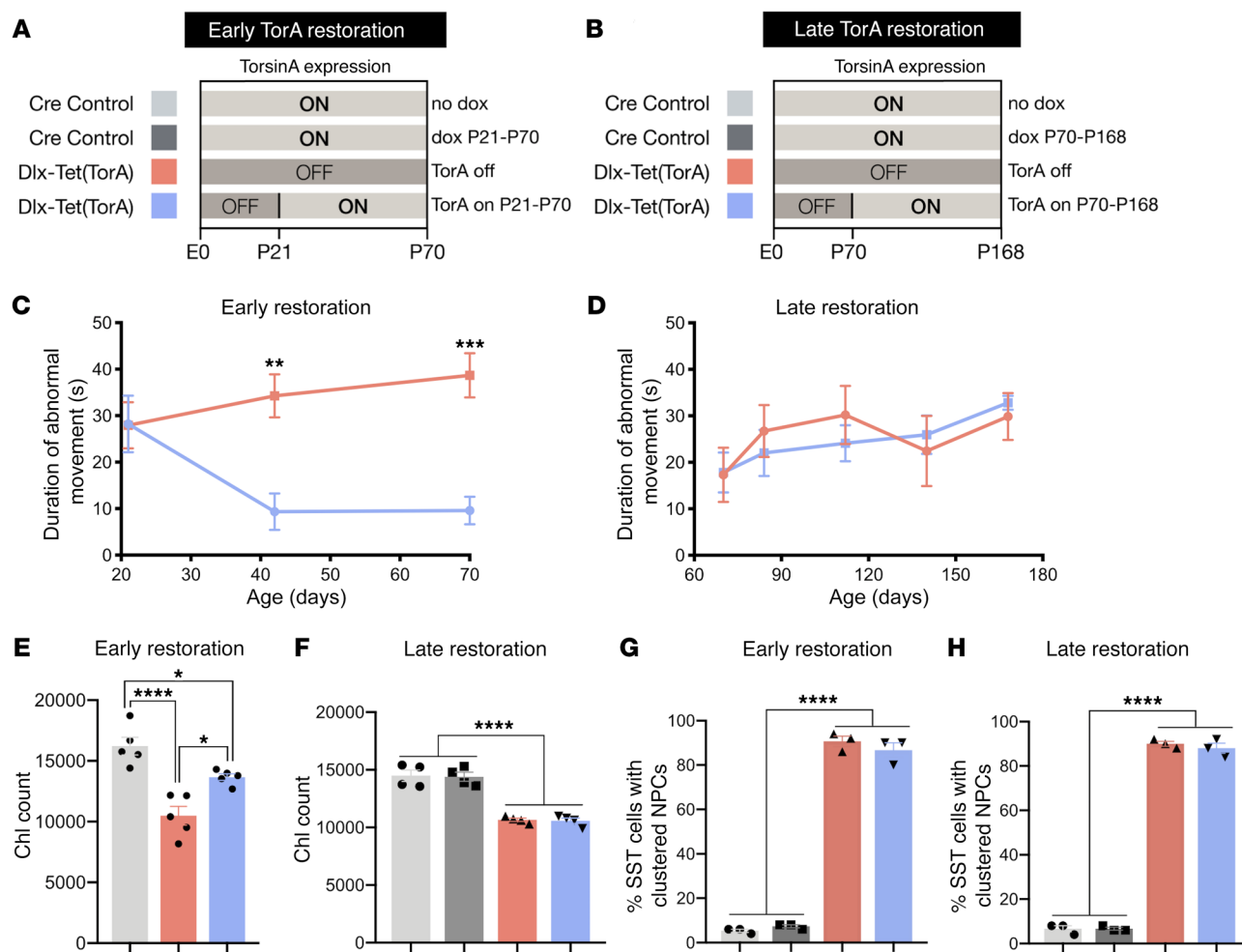
**Figure 5. Whole CNS torsinA depletion causes neuropathology only when initiated during CNS development.** (**A**) Representative Nissl-stained sagittal sections from P8 Nes-Tet(TorA) mice after prenatal suppression of torsinA. Scale bar: 500 μm. (**B**) Representative sagittal sections from P8 Nes-Tet(TorA) mice after prenatal suppression of torsinA immunostained with an antibody targeted to GFAP. Arrows indicate cortical gliosis and the circle outlines gliosis in thalamus. Scale bar: 500 μm. (**C**) GFAP fluorescence intensity analysis of P8 Nes-Tet(TorA) mice after prenatal suppression of torsinA. GFAP intensity increased in DCN, 7N, RN, thalamus, and cortex. $n = 3$ per group. (**D**) Schematic of experimental design for adult suppression of torsinA in the Nestin-Cre field. Light gray (ON) bars represent ages when torsinA is expressed and dark gray (OFF) areas represent ages when torsinA is suppressed. Each color corresponds to an experimental group in subsequent graphs. (**E**) Representative Nissl and GFAP costained sagittal sections from Nes-Tet(TorA) mice after adult suppression of torsinA. Scale bar: 1 mm. (**F**) GFAP fluorescence intensity analysis of P250 Nes-Tet(TorA) mice after adult suppression of torsinA. GFAP intensity is unchanged by adult torsinA suppression in all brain regions examined. $n = 5$ per group. (**G**) Cell counts of medial DCN neurons in P250 Nes-Tet(TorA) mice after adult suppression of torsinA. $n = 5$ per group. (**H**) Cell counts of 7N neurons in P250 Nes-Tet(TorA) mice after adult suppression of torsinA. $n = 5$ per group. Data analyzed by unpaired $t$ test (**C**) and 2-way ANOVA (**F–H**). *$P < 0.05$, **$P < 0.01$, ***$P < 0.001$.

**Figure 6. TorsinA restoration is uniquely effective during a neurodevelopmental therapeutic critical period.** (**A**) Schematic of experimental design for Dlx5/6-Cre juvenile torsinA restoration study. Light gray (ON) bars represent ages when torsinA is expressed and dark gray (OFF) areas represent ages when torsinA is suppressed. Each color corresponds to an experimental group in subsequent graphs. TorsinA expression was restored in early symptomatic Dlx-Tet(TorA) mice at P21. (**B**) Schematic of experimental design for Dlx-Tet(TorA) adult torsinA restoration study. Light gray (ON) bars represent ages when torsinA is expressed and dark gray (OFF) areas represent ages when torsinA is suppressed. Each color corresponds to an experimental group in subsequent graphs. TorsinA expression was restored in late symptomatic Dlx-Tet(TorA) mice at P70. (**C**) Duration of abnormal movements during 1 minute of tail suspension in Dlx-Tet(TorA) juvenile torsinA restoration mice. *n* = 9 per group. (**D**) Duration of abnormal movements during 1 minute of tail suspension in Dlx-Tet(TorA) adult torsinA restoration mice. *n* = 6 per group. (**E**) Striatal ChI counts in Dlx-Tet(TorA) juvenile torsinA restoration mice. TorsinA activation in juvenile mice partially prevents ChI degeneration. *n* = 5 per group. (**F**) Striatal ChI counts in Dlx-Tet(TorA) adult torsinA restoration mice. TorsinA activation in adult mice does not prevent ChI degeneration. *n* = 4 per group. (**G**) Percent of SST+ neurons with abnormally clustered nuclear pore complexes in sensorimotor cortex of Dlx-Tet(TorA) juvenile torsinA restoration mice. Juvenile torsinA activation does not rescue abnormal nuclear pore clustering. (**H**) Percentage of SST+ neurons with abnormally clustered nuclear pore complexes in sensorimotor cortex of Dlx-Tet(TorA) adult torsinA restoration mice. Adult torsinA activation does not rescue abnormal nuclear pore clustering. *n* = 3 per group. Data analyzed by 2-way ANOVA (**C**, **D**, and **F**–**H**) with Sidak's multiple-comparison test (**C**, **F**–**H**) and 1-way ANOVA with Tukey's multiple-comparison test (**E**). *$P < 0.05$, **$P < 0.01$, ***$P < 0.001$, ****$P < 0.0001$.

eration selectively after P21 expression of torsinA is consistent with the established timeline of ChI loss, which begins at approximately P12 and is complete by P70 or earlier (12). As with Dlx-CKO mice (23), Dlx-Tet(TorA) mice not treated with DOX exhibited nuclear pore clustering in SST+ cortical GABAergic interneurons. This phenotype was not reversed by induction of torsinA expression at either P21 or P70 (Figure 6, G and H). These results demonstrate that early torsinA augmentation halted ongoing loss of ChI and rescued motor abnormalities, strengthening the correlation between ChI dysfunction and abnormal twisting (12). These findings also establish a therapeutic critical period during CNS maturation.

The lack of benefit from torsinA augmentation in adulthood suggests that after early rescue, continued torsinA expression may not be required to maintain improved motor function and ChI integrity (Figure 6, C and E). We tested this possibility by comparing 4 experimental groups: 1. Dlx-Tet(TorA) mice with continuous torsinA suppression (Dlx-Tet[TorA][OFF]); 2. Dlx-Tet(TorA) mice with torsinA activated from P21 until the end of the study (Dlx-Tet[TorA][ON21-168]); 3. Dlx-Tet(TorA) mice with torsinA expressed from P21 to P70, then suppressed until the end of the study (Dlx-Tet[TorA][ON21-70]); and 4. *Cre* controls (Figure 7A). At P168, striatal lysates from Dlx-Tet(TorA)[OFF] and Dlx-Tet(TorA)[ON21-70]
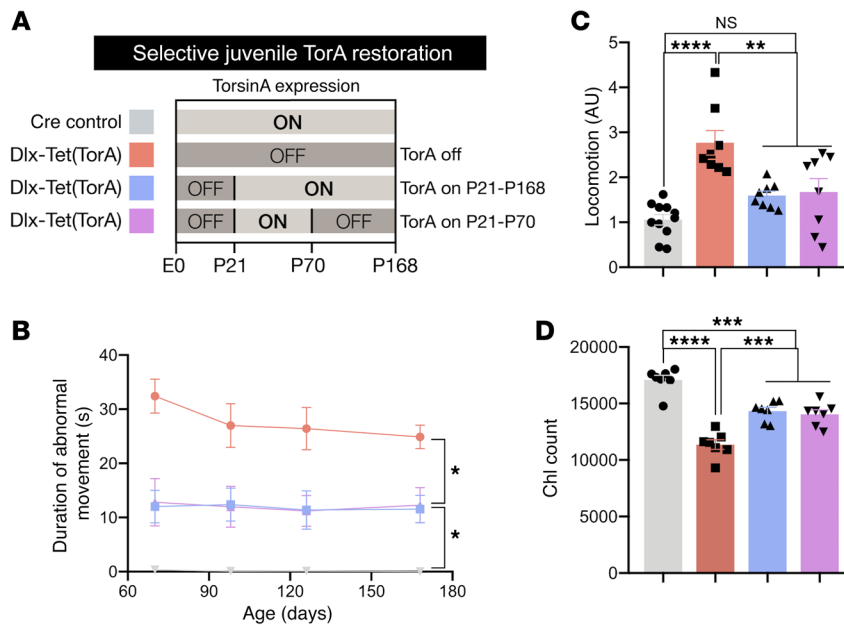
**Figure 7. TorsinA expression is not required after P70 to maintain early therapeutic rescue.** (**A**) Schematic of experimental design for Dlx-Tet(TorA) therapeutic critical period study. Light gray (ON) bars represent ages when torsinA is expressed and dark gray (OFF) areas represent ages when torsinA is suppressed. Each color corresponds to an experimental group in subsequent graphs. To determine whether ongoing torsinA expression in adulthood is necessary for persistent symptom amelioration, we compared Dlx-Tet(TorA) mice in which torsinA was not expressed (red; Dlx-Tet(TorA[OFF])), expressed from P21 to the end of the study (blue; Dlx-Tet(TorA)[ON21-168]), and expressed only from P21 to P70 (magenta; Dlx-Tet(TorA)[ON21-70]), and then suppressed from P70 to the end of the study at P168. (**B**) Duration of abnormal movements during 1 minute of tail suspension in Dlx-Tet(TorA) mice after torsinA repletion during a critical therapeutic period. $n = 8–12$ per group. (**C**) Locomotor activity in Dlx-Tet(TorA) mice after torsinA repletion during a critical therapeutic period. Reduction of hyperactivity in torsinA rescued mice persists to at least P168 even without ongoing adult torsinA expression. $n = 8–11$ per group. (**D**) Striatal ChI counts in Dlx-Tet(TorA) mice after torsinA repletion during a critical therapeutic period. TorsinA activation at P21 prevents striatal ChI degeneration, and no further degeneration occurs even when torsinA is inactivated at P70. $n = 7$ per group. Data analyzed by 2-way ANOVA with Sidak's multiple-comparison test (**B**) and 1-way ANOVA with Tukey's multiple-comparison test (**C** and **D**). *$P < 0.05$, **$P < 0.01$, ***$P < 0.001$, ****$P < 0.0001$.

mice showed similarly suppressed levels of torsinA, whereas Dlx-Tet(TorA)[ON21-168] mice with torsinA activated through the end of the study exhibited normal striatal torsinA expression (Supplemental Figure 13, A and B).

We performed behavioral testing from P70 to P168 followed by histological assessment. Tail suspension testing at P70 confirmed our earlier finding that torsinA activation from P21 to P70 significantly reversed motor symptoms (Figure 7B, first time point; compare with Figure 6C). Within the same group of mice (Dlx-Tet(TorA)[ON21-70] group; Figure 7B), this significant reduction in the duration of limb clasping persisted even 14 weeks after DOX cessation (torsinA suppressed). aIndeed, there was no significant difference in the duration of clasping between Dlx-Tet(TorA)[ON21-70] and Dlx-Tet(TorA)[ON21-168] (average time clasping: 12.3 seconds vs. 11.5 seconds), highlighting the lack of additional behavioral benefit from torsinA expression beyond P70. TorsinA activation at P21 also reversed hyperactivity at P168 whether or not torsinA expression was supported after P70 (Figure 7C). Stereological assessment of ChIs further supported the link between these cells and motor dysfunction. ChI numbers were rescued to a similar extent in both Dlx-Tet(TorA)[ON21-168] and Dlx-Tet(TorA)[ON21-70] groups (mean of control group = 17,082 cells; Dlx-Tet(TorA)[OFF] = 11,363 cells; Dlx-Tet(TorA)[ON21-168] = 14,330 cells; Dlx-Tet(TorA)[ON21-70] = 14,049 cells; Figure 7D). Considered together, these data demonstrate that torsinA expression was required exclusively during a critical period

before P70 to reverse DYT1-associated phenotypes. TorsinA supplementation beyond P70 was of no benefit either behaviorally or histopathologically.

## Discussion

Our studies are the first, to our knowledge, to establish a neurodevelopmental critical period during which the CNS is uniquely sensitive to torsinA function. Employing a genetic system to regulate expression of the endogenous *Tor1a* allele, we demonstrate an essential neurodevelopmental requirement for torsinA in supporting normal CNS structure and motor function that is dispensable in adult animals. We also demonstrate an analogous therapeutic critical period during which torsinA function must be restored to rescue the behavioral and neuropathological phenotypes caused by torsinA hypofunction. Our findings support a 2-stage model of disease pathogenesis. Stage 1 events are directly or closely related to torsinA LOF and reversible by torsinA restoration. Stage 2 events, by contrast, are downstream molecular or circuit changes that are independent of torsinA function. This model has broad implications for defining key molecular events relevant to neurodevelopmental disease pathogenesis and for the timing and nature of effective therapeutic strategies.

Modeling DYT1 dystonia is challenging because construct-valid (Tor1a[ΔE/+]) mice do not exhibit clear behavioral or neuropathological phenotypes (17, 22). Based on extensive biochemi-

cal, cell biological, and genetic evidence that the DYT1 mutation impairs torsinA function, we modeled the disease by deleting torsinA fully from corticostriatal circuits implicated in dystonia pathophysiology. Two caveats attend this approach. It almost certainly creates less torsinA enzymatic activity than the human DYT1 genotype, similar to how a transgenic modeling approach amplifies the effect of gain-of-function mutations. This approach also focuses exclusively on modeling torsinA LOF forebrain dysfunction (29). Although dysfunction of corticostriatal circuits is strongly implicated in dystonia, this approach omits potential contribution from the wider motor circuit, including the cerebellum, thalamus, and other regions (25, 39–43). Despite these caveats, our results demonstrate the necessity of torsinA function during a critical developmental period in all brain areas assessed (i.e., using both *Nestin-Cre* and *Dlx5/6-Cre*). This developmental selectivity is similar to the childhood-onset critical period in DYT1 dystonia subjects (15), supporting the disease relevance of these findings. These findings are also relevant to recessive loss of torsinA function recently linked to arthrogryposis (44, 45).

We demonstrate that torsinA restoration in juvenile (P21) mice that had been symptomatic for approximately 1 week (one-third of their lives) rescued motor symptoms and ChI degeneration. In contrast, gene replacement in stably symptomatic adult mice had no apparent effect. These data indicate that, over time, circuit dysfunction causing motor symptoms becomes torsinA-independent. This idea is consistent with the finding that in P21-rescued Dlx-Tet(TorA) mice, torsinA expression beyond P70 confers no further benefit. Changes not amenable to torsinA repletion likely include ChI degeneration because initiating torsinA replacement after ChI loss is ineffective. An association between prevention of ChI degeneration and behavioral rescue has been demonstrated in torsinA LOF models (46, 47), further supporting this connection. Striatal dysfunction secondary to ChI loss and dysfunction likely causes additional abnormalities of connectivity and function within and beyond the striatum, and failure to restore torsinA in these other neural elements may in part account for the incomplete motor rescue we observed. An important future direction for this work is to more resolutely define the time course and anatomical requirements for effective versus ineffective therapy.

Our studies of Dlx-Tet(TorA) mice add to a growing literature demonstrating striatal cholinergic abnormalities in dystonia. Striatal ChIs exhibit morphological, neurochemical, and electrophysiological changes in DYT1 dystonia mouse models (10, 12, 36, 38, 48, 49) and are linked to deficits in corticostriatal plasticity thought to contribute to the expression of motor symptoms (50, 51). In the Dlx-CKO model, ChIs are uniquely vulnerable to torsinA LOF (12). We found that torsinA activation early enough to prevent ChI degeneration rescued motor abnormalities, whereas torsinA activation in adult mice, after ChI degeneration was complete, did not improve the motor phenotype. These findings are consistent with another recent study demonstrating an association between ChI survival and motor symptoms (46), further strengthening the relationship between striatal cholinergic dysfunction and dystonic-like movements. However, other cells lack torsinA in Dlx-CKO mice, and selective degeneration of ChIs does not imply that they are the only key player. Other neuron populations in the Cre field, including cortical inhibito-

ry interneurons and striatal fast-spiking interneurons, have been implicated in dystonia pathophysiology (30–32). Future work will be needed to establish a causal link between ChI dysfunction and abnormal behavior and to explore whether dysfunction in other cell types contributes to motor dysfunction.

TorsinA LOF may dysregulate developmental plasticity through interactions with diverse pathways in which it has been implicated, including eIF2α signaling (52–54), secretory processing (55, 56), and nucleocytoplasmic transport (23, 57, 58). Manipulation of eIF2α signaling restores normal corticostriatal plasticity in brain slices from *Tor1a^{ΔE/+}* knockin mice (54). The secreted neurotrophic factor BDNF has also been linked to aberrant plasticity in *Tor1a^{ΔE/+}* mice (37). Pharmacological manipulation of BDNF signaling rescues plasticity deficits in juvenile mice (P26) but not adult mice, consistent with a therapeutic critical period for this intervention.

The biology of the torsin gene family provides clues to the mechanisms dictating a critical period of vulnerability in DYT1 dystonia. The torsinA paralog torsinB is developmentally regulated and strongly influences the severity of torsinA LOF phenotypes (24, 46, 59). Abnormal nuclear envelope budding occurs when torsinB expression is relatively low in the developing brain. This abnormal phenotype resolves as torsinB levels rise during maturation, but conversely persists and worsens when torsinA and torsinB are both ablated (24). TorsinB overexpression prevents torsinA LOF-related motor phenotypes and neurodegeneration (46). Studies of torsinB expression in humans are limited and inconclusive (60, 61), representing an important area of future investigation.

TorsinA action at the nuclear envelope may also regulate critical period timing. The number of NPCs in neurons increases rapidly during development before plateauing (62), and turnover of NPCs is exceedingly low (63, 64). TorsinA LOF results in abnormal NE budding in neurons (17), and this phenomenon appears related to interphase nuclear pore biogenesis. Nuclear pore components have been observed within NE buds, and the spatial characteristics of NE buds resemble those of nuclear pore complex intermediates (65). Further, torsinA-deficient neurons exhibit nuclear pore structures that appear incomplete, as they contain early NPC components but lack later-added nucleoporins present in mature nuclear pores (23, 66). This discrete developmental period of upregulated interphase nuclear pore insertion may be sensitive to torsinA function.

A report of motor abnormalities after shRNA-mediated torsinA knockdown in the cerebellum (39) of adult but not early postnatal animals differs from our finding of an early critical period for torsinA depletion (including for the cerebellum; Figure 4 and Figure 5). In contrast to the specific targeted approach employed here, the potential for off-target effects arising from multiple mechanisms in RNAi experiments may affect the shRNA findings (67–71). Indeed, our results are consistent with the natural history of the human disease (15), the multiple developmental processes described above in which torsinA has been implicated, and the presence of early motor abnormalities in multiple gene-targeted DYT1 and DYT6 models (12, 25, 72)

While it is important to bear in mind the many differences between mouse models and human disease, our observation of a therapeutic critical period for torsinA restoration has sig-

nificant translational implications. Our results suggest that for maximal efficacy, such therapies may need to be initiated early in pathogenesis. The ideal scenario is to identify and treat mutation carriers prior to symptom onset. This approach is not currently viable for DYT1 dystonia because the mutation is incompletely penetrant and there are no reliable predictors of which carriers will develop disease. In contrast, a torsinA-independent circuit-based approach will likely be required for patients with long-established symptoms. Current symptomatic treatments include pharmacological agents (e.g., antimuscarinics), botulinum toxin injection for focal symptoms, and deep brain stimulation (73). An alternative idea, suggested by our work, is modulating the torsinA critical period to impede disease pathophysiology or to make circuits more receptive to torsinA restoration. Several experimental interventions have been shown to extend critical periods or reactivate juvenile-like plasticity in adulthood (74, 75). Because DYT1 symptoms emerge during juvenile CNS maturation, critical period lengthening could worsen symptoms. Consistent with this possibility, aberrant plasticity is believed to be a core feature of dystonia pathophysiology (76–79). These considerations indicate that blocking defined plasticity pathways is also worthy of future study.

The identification of a therapeutic critical period for gene replacement is consistent with findings in mouse models of some but not all neurodevelopmental disorders. Early disruption or restoration of gene function is necessary to model or rescue behavioral phenotypes in mouse models of Angelman syndrome (1, 6). In contrast, the Rett syndrome protein *MeCP2* plays an essential role in maintenance of normal adult nervous system function (5, 80). Juvenile and adult *MeCP2* restoration ameliorate neurological dysfunction in Rett syndrome models with similar effectiveness (7). Similarly, in a *Shank3* mouse model of autism, adult replacement of the gene is sufficient to reverse synaptic deficits and improves autism-related behaviors (81). Neurodevelopmental diseases therefore differ in terms of the extent that the pathogenic process is uniquely required to occur during CNS maturation.

This is the first report, to our knowledge, establishing developmental and therapeutic critical periods in DYT1 dystonia. Our findings emphasize that future studies of torsinA pathways relevant to dystonia pathogenesis should focus on events that are unique to or strongly upregulated in maturing neurons. These experiments also suggest that torsinA-based therapeutic strategies can be effective even after symptoms have emerged, but likely need to be administered early in the course of disease.

## Methods

### Mice
The Tet(TorA) mouse line was generated with Biocytogen using CRISPR/Extreme Genome Editing technology. A floxed stop cassette and TetO sequence were inserted upstream of *Tor1a* exons 1–5. For more information, please refer to Supplemental Methods.

### Western blotting
PVDF membranes were probed with rabbit anti-torsinA (Abcam, ab34540; 1:10,000) and rabbit anti-calnexin (Enzo Life Sciences, SPA-860; 1:20,000) primary antibodies. The secondary antibody

was an HRP-conjugated anti-rabbit antibody (Cell Signaling Technology, 7074; 1:20,000). Bands were visualized using chemiluminescent substrate and exposure to x-ray film. Protein levels were quantified in ImageJ (NIH). For more information, please refer to Supplemental Methods.

### Immunohistochemistry
For immunofluorescence, 40 μm free-floating brain sections were incubated with rabbit anti-GFAP (Dako, Z0334; 1:2,000), rabbit anti-SST (Abcam, ab103790; 1:500), and/or mouse anti–nuclear pore complex (mAb414; Abcam, ab24609; 1:800) primary antibodies. This was followed by incubation with donkey anti-rabbit Ax555 secondary antibody (Invitrogen, A-31572; 1:800), donkey anti-mouse Ax488 secondary antibody (Invitrogen, A-21206), Hoechst (Thermo Fisher Scientific, 62249; 1:10,000), and/or NeuroTrace green fluorescent Nissl stain (Invitrogen, N21380). Sections were mounted on glass slides and cover-slipped with ProLong Gold mounting medium (Invitrogen, P36930). For DAB staining, 40 μm fixed sections were stained with goat anti-ChAT (MilliporeSigma, AB144P; 1:800) primary antibody, followed by incubation with biotinylated donkey anti-goat secondary antibody (Jackson ImmunoResearch, 705-06547; 1:800), ABC-HRP kit (Vector Laboratories, PK-6100), and DAB substrate (Sigma-Aldrich, D4293; 3,3′-diaminobenzidine). For traditional Nissl staining, 40 μm fixed brain sections were mounted on glass slides, rehydrated, incubated in Cresyl violet for 3 minutes, and quenched in water. After Nissl or DAB staining, sections were dehydrated in ascending ethanols, cleared in xylenes, and cover-slipped with Permount mounting medium (Thermo Fisher Scientific, SP15). For more information, please refer to Supplemental Methods.

### Cell counting and image analysis
*Stereology.* ChIs, striatal neurons, 7N neurons, and medial deep cerebellar nuclei neurons were quantified with unbiased stereology using the optical fractionator probe in Stereoinvestigator (MBF Bioscience). Forty-micrometer-thick serial sections were observed using a Zeiss Axioimager M2 microscope. Counting frame and sampling grid parameters were determined in pilot studies to reach a Gundersen coefficient of error of less than 0.1 for each cell type/region. For more information, please refer to Supplemental Methods.

*Morphological analysis.* Cortical thickness and striatal volume were measured as previously described (12). Brain area was measured in sagittal sections by creating a contour around the brain in the section corresponding to mediolateral +1.44 mm (82) and measuring the traced area in Stereoinvestigator.

*Image analysis.* Glial fibrillary acidic protein (GFAP) fluorescence intensity was measured in ImageJ by creating a region of interest around the specific brain regions and quantifying fluorescence intensity in the GFAP channel. NPC clustering was scored (yes or no) in SST+ interneurons in the motor cortex by a reviewer blinded to genotype.

### Behavioral testing
*Tail suspension.* Mice were suspended by the tail and recorded for 60 seconds. Two scorers blinded to genotype graded the presence of abnormal clasping and twisting movements as well as the duration of abnormal movements.

*Locomotor activity.* Mice were placed individually into a plastic mouse cage (18 cm × 28 cm) with a thin layer of bedding. The cage

was placed into a dark plexiglass box, and locomotor activity was measured by photobeams (Photobeam Activity System, San Diego Instruments). Horizontal beam breaks were recorded for 1 hour.

*Rotarod*. Mice were tested on an accelerating rotarod with the speed of rotation increasing from 4 to 40 rpm over 5 minutes. Latency to fall was recorded with a cutoff of 5 minutes. Five trials were conducted per day for 2 consecutive days, with 2 minutes of rest between trials.

*Kyphosis*. Mice were observed in an empty cage for 2 minutes. Presence or absence of abnormal spinal kyphosis was noted by a reviewer blinded to the experimental group of the mice.

*Video tracking*. Mice were recorded for 10 minutes by a camera above an open field environment (44 × 44 cm, walls 30 cm high). Two reviewers blinded to the experimental group of each mouse scored videos for the presence or absence of overt dystonic postures observed in other dystonia models (39, 83, 84). These included difficulty maintaining balance, erratic gait, and other dystonic postures.

### Statistics
Statistical testing and graph generation were performed using Graph-Pad Prism software. Data are represented as mean ± SEM. Descriptions of statistical tests and sample sizes are located in figure legends. $P$ values less than 0.05 were considered significant.

### Study approval
Animal work described in this manuscript has been approved and conducted under the oversight of the University of Texas Southwestern and University of Michigan IACUCs.

## Author contributions
JL, SSP, and WTD designed research studies. JL, DSL, and AJK conducted experiments, acquired data, and analyzed data. JL, SSP, and WTD wrote and edited the manuscript.

## Acknowledgments

Address correspondence to: William T. Dauer, 6000 Harry Hines Blvd., NB5.604, Dallas, Texas 75390-8823, USA. Phone: 214.645.3332; Email: william.dauer@utsouthwestern.edu. Or to: Samuel S. Pappas, 6001 Forest Park Rd., Dallas, Texas 75390-8823, USA. Phone: 214.645.3339; Email: samuel.pappas@utsouthwestern.edu.

1. Sonzogni M, et al. Delayed loss of UBE3A reduces the expression of Angelman syndrome-associated phenotypes. *Mol Autism*. 2019;10:23.
2. Ikonomidou C, et al. Ethanol-induced apoptotic neurodegeneration and fetal alcohol syndrome. *Science*. 2000;287(5455):1056–1060.
3. Tenkova T, et al. Ethanol-induced apoptosis in the developing visual system during synaptogenesis. *Invest Ophthalmol Vis Sci*. 2003;44(7):2809–2817.
4. Kariya S, et al. Requirement of enhanced Survival Motoneuron protein imposed during neuromuscular junction maturation. *J Clin Invest*. 2014;124(2):785–800.
5. Nguyen MV, et al. MeCP2 is critical for maintaining mature neuronal networks and global brain anatomy during late stages of postnatal brain development and in the mature adult brain. *J Neurosci*. 2012;32(29):10021–10034.
6. Silva-Santos S, et al. Ube3a reinstatement identifies distinct developmental windows in a murine Angelman syndrome model. *J Clin Invest*. 2015;125(5):2069–2076.
7. Guy J, et al. Reversal of neurological defects in a mouse model of Rett syndrome. *Science*. 2007;315(5815):1143–1147.
8. Bhatia KP, Marsden CD. The behavioural and motor consequences of focal lesions of the basal ganglia in man. *Brain*. 1994;117(pt 4):859–876.
9. Carbon M, et al. Regional metabolism in primary torsion dystonia: effects of penetrance and genotype. *Neurology*. 2004;62(8):1384–1390.
10. Martella G, et al. Impairment of bidirectional synaptic plasticity in the striatum of a mouse model of DYT1 dystonia: role of endogenous acetylcholine. *Brain*. 2009;132(pt 9):2336–2349.
11. Eskow Jaunarajs KL, et al. Striatal cholinergic dysfunction as a unifying theme in the pathophysiology of dystonia. *Prog Neurobiol*. 2015;127–128:91–107.
12. Pappas SS, et al. Forebrain deletion of the dystonia protein torsinA causes dystonic-like movements and loss of striatal cholinergic neurons. *Elife*. 2015;4:e08352.
13. Akbari MT, et al. Clinical features, DYT1 mutation screening and genotype-phenotype correlation in patients with dystonia from Iran. *Med Princ Pract*. 2012;21(5):462–466.
14. Albanese A, et al. EFNS guidelines on diagnosis and treatment of primary dystonias. *Eur J Neurol*. 2011;18(1):5–18.
15. Bressman SB, et al. The DYT1 phenotype and guidelines for diagnostic testing. *Neurology*. 2000;54(9):1746–1752.
16. Ozelius LJ, et al. The early-onset torsion dystonia gene (DYT1) encodes an ATP-binding protein. *Nat Genet*. 1997;17(1):40–48.
17. Goodchild RE, et al. Loss of the dystonia-associated protein torsinA selectively disrupts the neuronal nuclear envelope. *Neuron*. 2005;48(6):923–932.
18. Naismith TV, et al. Interaction of torsinA with its major binding partners is impaired by the dystonia-associated DeltaGAG deletion. *J Biol Chem*. 2009;284(41):27866–27874.
19. Demircioglu FE, et al. Structures of TorsinA and its disease-mutant complexed with an activator reveal the molecular basis for primary dystonia. *Elife*. 2016;5:e17983.
20. Zhao C, et al. Activation of Torsin ATPases. *Proc Natl Acad Sci U S A*. 2013;110(17):E1545–E1554.
21. Brown RSH, et al. Mechanism of Torsin ATPase activation. *Proc Natl Acad Sci U S A*. 2014;111(45):E4822–E4831.
22. Tanabe LM, et al. Genetic background modulates the phenotype of a mouse model of DYT1 dystonia. *PLoS One*. 2012;7(2):e32245.
23. Pappas SS, et al. TorsinA dysfunction causes persistent neuronal nuclear pore defects. *Hum Mol Genet*. 2018;27(3):407–420.
24. Tanabe LM, et al. Neuronal nuclear membrane budding occurs during a developmental window modulated by torsin paralogs. *Cell Rep*. 2016;16(12):3322–3333.
25. Liang CC, et al. TorsinA hypofunction causes abnormal twisting movements and sensorimotor circuit neurodegeneration. *J Clin Invest*. 2014;124(7):3080–3092.
26. Weisheit CE, Dauer WT. A novel conditional knock-in approach defines molecular and circuit effects of the DYT1 dystonia mutation. *Hum Mol Genet*. 2015;24(22):6459–6472.
27. Tanaka KF, et al. Flexible Accelerated STOP Tetracycline Operator-knockin (FAST): a versatile and efficient new gene modulating system. *Biol Psychiatry*. 2010;67(8):770–773.
28. Freundlieb S, et al. A tetracycline controlled activation/repression system with increased potential for gene transfer into mammalian cells. *J Gene Med*. 1999;1(1):4–12.
29. Monory K, et al. The endocannabinoid system controls key epileptogenic circuits in the hippocampus. *Neuron*. 2006;51(4):455–466.
30. Ridding MC, et al. Changes in the balance between motor cortical excitation and inhibition in focal, task specific dystonia. *J Neurol Neurosurg Psychiatry*. 1995;59(5):493–498.
31. McDonnell MN, et al. The effect of cutaneous input on intracortical inhibition in focal task-specific dystonia. *Mov Disord*. 2007;22(9):1286–1292.
32. Gittis AH, et al. Selective inhibition of striatal fast-spiking interneurons causes dyskinesias. *J Neurosci*. 2011;31(44):15727–15731.
33. Mallo M, et al. Reversible gene inactivation in the

mouse. *Genomics*. 2003;81(4):356–360.

34. Krauss JK, et al. Dystonia following head trauma: a report of nine patients and review of the literature. *Mov Disord*. 1992;7(3):263–272.

35. Prell T, et al. Structural brain abnormalities in cervical dystonia. *BMC Neurosci*. 2013;14:123.

36. Maltese M, et al. Anticholinergic drugs rescue synaptic plasticity in DYT1 dystonia: role of M1 muscarinic receptors. *Mov Disord*. 2014;29(13):1655–1665.

37. Maltese M, et al. Early structural and functional plasticity alterations in a susceptibility period of DYT1 dystonia mouse striatum. *Elife*. 2018;7:e33331.

38. Pappas SS, et al. A cell autonomous torsinA requirement for cholinergic neuron survival and motor control. *Elife*. 2018;7:e36691.

39. Fremont R, et al. A role for cerebellum in the hereditary dystonia DYT1. *Elife*. 2017;6:e22775.

40. Shakkottai VG, et al. Current opinions and areas of consensus on the role of the cerebellum in dystonia. *Cerebellum*. 2017;16(2):577–594.

41. Tasker RR, et al. Thalamotomy in generalized dystonia. *Adv Neurol*. 1988;50:615–631.

42. Neychev VK, et al. The functional neuroanatomy of dystonia. *Neurobiol Dis*. 2011;42(2):185–201.

43. Prudente CN, et al. Dystonia as a network disorder: what is the role of the cerebellum? *Neuroscience*. 2014;260:23–35.

44. Reichert SC, et al. Biallelic TOR1A variants in an infant with severe arthrogryposis. *Neurol Genet*. 2017;3(3):e154.

45. Isik E, et al. Biallelic TOR1A mutations cause severe arthrogryposis: A case requiring reverse phenotyping. *Eur J Med Genet*. 2019;62(9):103544.

46. Li J, et al. TorsinB overexpression prevents abnormal twisting in DYT1 dystonia mouse models. *Elife*. 2020;9:e54285.

47. Cascalho A, et al. Excess Lipin enzyme activity contributes to TOR1A recessive disease and DYT-TOR1A dystonia. *Brain*. 2020;143(6):1746–1765.

48. Sciamanna G, et al. Cholinergic dysregulation produced by selective inactivation of the dystonia-associated protein torsinA. *Neurobiol Dis*. 2012;47(3):416–427.

49. Song CH, et al. Subtle microstructural changes of the striatum in a DYT1 knock-in mouse model of dystonia. *Neurobiol Dis*. 2013;54:362–371.

50. Shen W, et al. M4 muscarinic receptor signaling ameliorates striatal plasticity deficits in models of L-DOPA-induced dyskinesia. *Neuron*. 2016;90(5):1139.

51. Wang Z, et al. Dopaminergic control of corticostriatal long-term synaptic depression in medium spiny neurons is mediated by cholinergic interneurons. *Neuron*. 2006;50(3):443–452.

52. Beauvais G, et al. Exploring the interaction between eIF2α dysregulation, acute endoplasmic reticulum stress and DYT1 dystonia in the mammalian brain. *Neuroscience*. 2018;371:455–468.

53. Beauvais G, et al. Disruption of protein processing in the endoplasmic reticulum of DYT1 knock-in mice implicates novel pathways in dystonia pathogenesis. *J Neurosci*. 2016;36(40):10245–10256.

54. Rittiner JE, et al. Functional genomic analyses of mendelian and sporadic disease identify impaired eIF2α signaling as a generalizable mechanism for dystonia. *Neuron*. 2016;92(6):1238–1251.

55. Hewett JW, et al. Mutant torsinA interferes with protein processing through the secretory pathway in DYT1 dystonia cells. *Proc Natl Acad Sci U S A*. 2007;104(17):7271–7276.

56. Hewett JW, et al. siRNA knock-down of mutant torsinA restores processing through secretory pathway in DYT1 dystonia cells. *Hum Mol Genet*. 2008;17(10):1436–1445.

57. VanGompel MJ, et al. A novel function for the Caenorhabditis elegans torsin OOC-5 in nucleoporin localization and nuclear import. *Mol Biol Cell*. 2015;26(9):1752–1763.

58. Rampello AJ, et al. Torsin ATPase deficiency leads to defects in nuclear pore biogenesis and sequestration of MLF2. *J Cell Biol*. 2020;219(6):e201910185.

59. Kim CE, et al. A molecular mechanism underlying the neural-specific defect in torsinA mutant mice. *Proc Natl Acad Sci U S A*. 2010;107(21):9861–9866.

60. Augood SJ, et al. Distribution of the mRNAs encoding torsinA and torsinB in the normal adult human brain. *Ann Neurol*. 1999;46(5):761–769.

61. Bahn E, et al. TorsinB expression in the developing human brain. *Brain Res*. 2006;1116(1):112–119.

62. Lodin Z, et al. Nuclear pore complexes in cells of the developing mouse cerebral cortex. *Acta Histochem*. 1978;63(1):74–79.

63. Toyama BH, et al. Identification of long-lived proteins reveals exceptional stability of essential cellular structures. *Cell*. 2013;154(5):971–982.

64. Dorrbaum AR, et al. Local and global influences on protein turnover in neurons and glia. *Elife*. 2018;7:e34202.

65. Laudermilch E, et al. Dissecting Torsin/cofactor function at the nuclear envelope: a genetic study. *Mol Biol Cell*. 2016;27(25):3964–3971.

66. Otsuka S, et al. Nuclear pore assembly proceeds by an inside-out extrusion of the nuclear envelope. *Elife*. 2016;5:e19071.

67. Jackson AL, et al. Expression profiling reveals off-target gene regulation by RNAi. *Nat Biotechnol*. 2003;21(6):635–637.

68. Jackson AL, et al. Widespread siRNA "off-target" transcript silencing mediated by seed region sequence complementarity. *RNA*. 2006;12(7):1179–1187.

69. Jackson AL, Linsley PS. Recognizing and avoiding siRNA off-target effects for target identification and therapeutic application. *Nat Rev Drug Discov*. 2010;9(1):57–67.

70. Adamson B, et al. A genome-wide homologous recombination screen identifies the RNA-binding protein RBMX as a component of the DNA-damage response. *Nat Cell Biol*. 2012;14(3):318–328.

71. Schultz N, et al. Off-target effects dominate a large-scale RNAi screen for modulators of the TGF-β pathway and reveal microRNA regulation of TGFBR2. *Silence*. 2011;2:3.

72. Yellajoshyula D, et al. The DYT6 dystonia protein THAP1 regulates myelination within the oligodendrocyte lineage. *Dev Cell*. 2017;42(1):52–67.

73. Cloud LJ, Jinnah HA. Treatment strategies for dystonia. *Expert Opin Pharmacother*. 2010;11(1):5–15.

74. Castren E, et al. Treatment of neurodevelopmental disorders in adulthood. *J Neurosci*. 2012;32(41):14074–14079.

75. Bavelier D, et al. Removing brakes on adult brain plasticity: from molecular to behavioral interventions. *J Neurosci*. 2010;30(45):14964–14971.

76. Altenmuller E, Jabusch HC. Focal dystonia in musicians: phenomenology, pathophysiology, triggering factors, and treatment. *Med Probl Perform Art*. 2010;25(1):3–9.

77. Edwards MJ, et al. Abnormalities in motor cortical plasticity differentiate manifesting and nonmanifesting DYT1 carriers. *Mov Disord*. 2006;21(12):2181–2186.

78. Gilbertson T, et al. Maladaptive striatal plasticity and abnormal reward-learning in cervical dystonia. *Eur J Neurosci*. 2019;50(7):3191–3204.

79. Quartarone A, et al. Abnormal plasticity of sensorimotor circuits extends beyond the affected body part in focal dystonia. *J Neurol Neurosurg Psychiatry*. 2008;79(9):985–990.

80. Du F, et al. Acute and crucial requirement for MeCP2 function upon transition from early to late adult stages of brain maturation. *Hum Mol Genet*. 2016;25(9):1690–1702.

81. Mei Y, et al. Adult restoration of Shank3 expression rescues selective autistic-like phenotypes. *Nature*. 2016;530(7591):481–484.

82. Franklin KBJ, Paxinos G. *Paxinos and Franklin's the Mouse Brain in Stereotaxic Coordinates*. Academic Press; 2013.

83. Calderon DP, et al. The neural substrates of rapid-onset Dystonia-Parkinsonism. *Nat Neurosci*. 2011;14(3):357–365.

84. Washburn S, et al. Acute cerebellar knockdown of *Sgce* reproduces salient features of myoclonus-dystonia (DYT11) in mice. *Elife*. 2019;8:e52101.